Optimization of Phased Array Coils for Small-animal MRI at 9.4T

Z. Wang[1], M. Tabbert[2], S. Junge[2], R. E. Gordon[2], Q. X. Yang[1], M. B. Smith[3], and C. M. Collins[1]

[1]Radiology, The Pennsylvania State University, Hershey, PA, United States, [2]BRUKER Biospin GmbH, Ettlingen, Germany, [3]Novartis Institutes for BioMedical Research, Inc., Boston, MA, United States

INTRODUCTION: Animal imaging with phased array coils in high field MRI has become increasingly routine [1,2]. Mice and rats are among the species most often imaged. To increase the SNR in comparison to existing standard quadrature birdcage coils and an existing phased array coil design [3], we have performed a numerical analysis and comparison of several proposed array geometries loaded with either a rat head or a mouse body considering the axial B1-homogeneity, B1-sensitivity and g-factor distribution. Based on the simulation results two different coil geometries were designed and comparisons of the coil performance were done on an MR-scanner.

METHOD: Phased array coils with different lengths were modeled using CST Microwave Studio (CST GmbH, Germany), including one row of coils from 4 to 16 elements, and two rows from 2x6 to 2x8 elements. Models of a cylindrical phantom, a rat head, and a mouse whole body were loaded for the comparison. Various representative models are shown in Fig. 1. The anatomically accurate rat head model consists of 11 different tissue types with a 0.5 mm isometric resolution, and was created by a manual segmentation of MRI data. The mouse is scaled from United States Air Force Research Laboratory rat model and contains 16 tissues. The g-factor was calculated for comparison of the different phase encoding direction and acceleration rate using standard methods [4]. Two different array coils consisting of 6 and 8 elements respectively were constructed for comparisons of the performance on an MR-scanner. The coils were designed on a FR4 cylindrical former. Each element of the array was decoupled by overlaps from the nearest neighbors and by transformers to the next elements respectively. All elements of the coils are equipped with an active-decoupling circuit and are decoupled additionally via preamplifier decoupling using low input-impedance preamplifiers (R_{input}=2.0 Ω, NF=0.5 dB, gain 27 dB) [5]. The elements of the coil array were matched and tuned stationary for a medium-sized load. All measurements of this study were performed on a ClinScan® 7T-Animal-System (Bruker BioSpin MRI GmbH, Ettlingen, Germany) equipped with 16 receive-channels and a 1.4kW transmit amplifier. The built-in body coil of the MR-scanner was used for excitation.

RESULTS AND DISCUSSION: The maximum g-factor values for one-row and two-row phased array coils are listed in Table I and II. For one-ring array coils, it is easy to see that more elements give better results, but for most cases eight elements gives a good compromise between maximum g-factor and coil complexity. The shorter coil also has lower g-factors, but less coverage. For two-ring array coils, the 2x8 type has notably better performance than 2x6, and the coil length of 45cm outperformed longer and shorter coils. The g-factor distribution of different phase encoding direction and acceleration rate for rat head are presented in Fig. 2. Because the effect of the ears, the horizontal phase encoding direction has better performance than the vertical direction, especially at high acceleration rates. The accelerated images of the MR-measurements are shown the predicted noise enhancements in regions of higher g-factors of the equivalent g-factor maps calculated by the simulations. Apart from the lower g-factors and less noise enhancements of the 8 channel array-coil, both coils work well up to an acceleration factor of 3 (Fig. 3). Depending on the decoupling performance between the array-coil elements the 8 channel array-coil (S_{12} > -20dB) shows a superior SNR and sensitivity distribution compared to the 6 channel array-coil.

ACKNOWLEDGMENT: Many Thanks to S. Widmaier, H. Lehr and C. Meier for acquiring the MR-images. Funded in part through NIH R01 EB006563.

REFERENCES: [1] FD Doty *et al.*, NMR Biomed.2007;20:304-325; [2] D Gareis *et al.*, NMR Biomed.2007;20:326-334; [3] MA. Lopez *et al.*, Proc. ISMRM, 2007, p. 1026; K Pruessmann *et al.*, Magn Reson Med 1999;42:952–962; [5] A. Reykowski, Magn Reson Med 1995;33: 848-852.

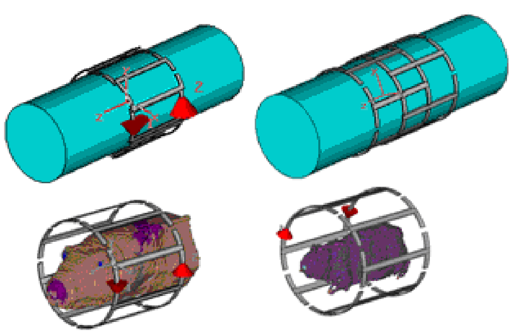

Figure 1 Some representative coil and animal geometries.

Table I Maximum g-factor with cylinder loaded in one-row array

Coil length (cm)	Acceleration Rate	Number of Coils					
		4	6	8	10	12	16
35	2	1.61	1.15	1.04	1.03	1.03	1.03
	3	7.22	2.70	1.50	1.39	1.34	1.28
	4	1568	7.21	3.88	2.60	2.39	2.13
40	2	1.61	1.17	1.04	1.04	1.04	1.03
	3	7.17	2.54	1.50	1.41	1.38	1.27
	4	1436	7.31	3.72	2.63	2.45	2.15

Table II Maximum g-factor with cylinder loaded in two-row array

Array Length (cm)	Acceleration Rate	2x6	2x8
35	2	1.13	1.04
	3	1.82	1.51
	4	4.11	2.85
45	2	1.12	1.04
	3	1.79	1.56
	4	4.13	2.92
55	2	1.15	1.05
	3	1.79	1.63
	4	4.03	3.06

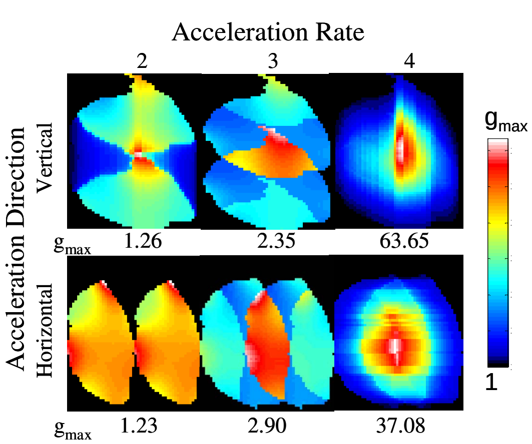

Figure 2 g-factor distribution in rat head model for 8-element, 35cm on-row array with different phase encoding direction and acceleration rates. Top of head is towards right of figure. Extension of ear cause very poor g-factors than seen for cylinder (Table I) at higher acceleration rates.

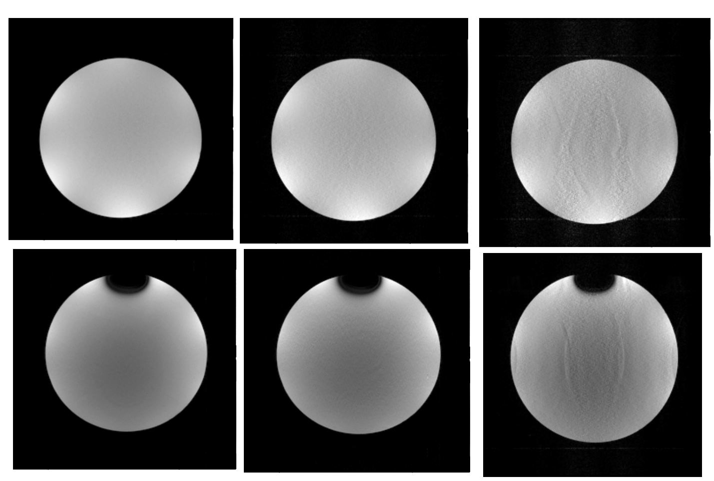

Figure 3. Accelerated Images (FLASH) acquired with a 6 Ch (top) and 8 Ch (bottom) array with acceleration rates of 2 (left), 3 (center), and 4 (right).